Parton equilibration in relativistic heavy ion collisions

T. S. Biró,[1,2] E. van Doorn,[1] B. Müller,[1] M. H. Thoma,[1,2] and X.-N. Wang[1,3]
[1]*Department of Physics, Duke University, Durham, North Carolina 27708*
[2]*Institut für Theoretische Physik, Universität Giessen, D-35392 Giessen, Germany*
[3]*Nuclear Science Division, Lawrence Berkeley Laboratory, Berkeley, California 94720*
(Received 5 March 1993)

We investigate the processes leading to phase-space equilibration of parton distributions in nuclear interactions at collider energies. We derive a set of rate equations describing the chemical equilibration of gluons and quarks including medium effects on the relevant QCD transport coefficients, and discuss their consequences for parton equilibration in heavy ion collisions.

PACS number(s): 25.75.+r, 12.38.Mh, 13.87.Ce, 24.85.+p

I. INTRODUCTION

The mechanisms that precede the formation of a thermalized, locally deconfined plasma of quarks and gluons in relativistic nuclear collisions have recently attracted considerable interest, because it was noticed that the preequilibrium phase may influence the yield of certain quark-gluon plasma signals, such as lepton pairs and hadrons containing heavy quarks. The space-time evolution of quark and gluon distributions has been investigated in the framework of the parton cascade model [1]. This model is based on the concept of the inside-outside cascade [2–4] and evolves parton distributions by Monte Carlo simulation of a relativistic transport equation involving lowest-order perturbative QCD scattering and parton fragmentation. Numerical studies [5,6] have shown that phase-space equilibration of partons occurs over a period of 1–2 fm/c, and is initially dominated by gluon-induced processes.

From these investigations, and from more schematic considerations, a picture involving three distinct stages of parton evolution has emerged [7–11]: (1) Gluons "thermalize" very rapidly, reaching approximately isotropic momentum space distributions after a time of the order of 0.3 fm/c. (2) Full equilibration of the gluon phase-space density takes considerably longer. (3) The evolution of quark distributions lags behind that of the gluons, because the relevant QCD cross sections are suppressed by a factor of 2–3.

Although this picture emerges from the numerical simulations of the parton cascade model [11], the complexity of these calculations makes it difficult to obtain a lucid understanding of the dependence of the different time scales on various parameters and model assumptions. It is the goal of our present investigation to derive this insight.

A second, equally important, motivation for our study was the desire to obtain a better physical understanding of the infrared cutoffs required in the parton cascade model. The two cutoff parameters employed in Ref. [1], the minimal transverse momentum transfer p_0 in binary parton interactions, and the infrared cutoff $z_{\min}$ in parton fragmentation processes were determined by comparison with cross sections and particle multiplicities measured in nucleon-nucleon interactions at high energies. These values are assumed to reflect the transition between the perturbative and nonperturbative regimes of QCD in the normal vacuum. On the other hand, it is well known that color screening provides a *natural* cutoff of long-range interactions in a deconfined QCD plasma [12], and no artificial cutoff parameters are required to obtain finite perturbative cross sections in a dense medium [13].

A previous study [14] has shown that screening effects may be sufficiently strong immediately after the primary parton collision events in nuclear collisions at the Brookhaven Relativistic Heavy Ion Collider (RHIC) energies and beyond to provide the infrared cutoff required in the treatment of secondary parton interactions. Improved understanding [15] of the suppression of fragmentation processes in a dense QCD plasma (Landau-Pomeranchuk effect) has also allowed one to regard the infrared cutoff $z_{\min}$ as a medium-dependent effect in relativistic nuclear collisions. We show here how these medium effects can be utilized to obtain a parameter-free set of equations, based on perturbative QCD in a dense partonic medium, that describes the evolution of quark and gluon distributions towards equilibrium. Arbitrary cutoff parameters enter only into the description of the primary semihard parton scattering, where one must continue to rely on a comparison with nucleon scattering data. After this short initial phase, however, the approach towards an equilibrated quark-gluon plasma will be described without the need for arbitrary parameters.

Our paper is structured as follows: Section II discusses initial parton production in relativistic nuclear collisions. The evolution of these partons into locally isotropic, quasithermal momentum distributions is described in Sec. III. In Sec. IV we derive a set of rate equations describing the further evolution and chemical equilibration of gluon and quark distributions. The influence of the dense medium on the relevant QCD cross sections is discussed in Sec. V, and a closed set of rate equations including these medium modifications is derived. We explore the solution of these equations in Sec. VI. Some consequences for quark-gluon plasma signatures are briefly discussed in the conclusions.

II. MINIJET PRODUCTION

In high energy nucleon-nucleon collisions the production of minijets with p_T about a few GeV becomes increasingly important at colliding energies beyond the CERN ISR energy range [16]. One would certainly expect that there could be a fairly large number of minijets produced in ultrarelativistic heavy ion collisions. It was estimated by Kajantie *et al.* [17] that minijets could contribute up to half of the total transverse energy produced in heavy ion collisions at RHIC energy. Unlike the soft processes which dominate the reaction at lower energies, those minijets carry relatively large transverse momenta and they quickly become incoherent from the rest of nuclear matter in the fragmentation region. If a sufficiently high density is reached and the equilibration proceeds rapidly, those minijets would eventually lead to a thermalized and locally deconfined quark gluon plasma.

To estimate the initial parton density, we calculate the minijet production using the HIJING Monte Carlo model [18]. In this model, perturbative QCD, implemented along the lines of the Monte Carlo event generator Pythia [19], is combined together with low p_T phenomenology to describe multiple minijet production in each binary nucleon-nucleon collision. One important quantity in the model is the inclusive jet cross section. Given the parton structure function $f_a(x, p_T^2)$ and the perturbative parton-parton cross section $d\sigma_{ab}$, the differential jet cross section in nucleon-nucleon collisions can be calculated as [20]

$$\frac{d\sigma_{\rm jet}}{dp_T^2 dy_1 dy_2} = K \sum_{a,b} x_1 f_a(x_1, p_T^2) x_2 f_b(x_2, p_T^2) \frac{d\sigma_{ab}}{d\hat{t}}, \quad (1)$$

where the phenomenological factor $K \approx 2$ accounts for higher-order corrections and x_1, x_2 are the Feynman variables denoting the longitudinal momentum fraction carried by a parton. Since this cross section diverges and the perturbative approach fails at small p_T, we introduce an infrared cutoff p_0 to calculate the total inclusive jet cross section $\sigma_{\rm jet}(p_0)$. Introducing $\sigma_{\rm soft}$ for the soft interactions below the cutoff, we obtain the inelastic cross section for nucleon-nucleon collisions in the eikonal approximation [21],

$$\sigma_{\rm in} = \int d^2b \left[1 - e^{-(\sigma_{\rm soft} + \sigma_{\rm jet}) T_N(b)}\right], \quad (2)$$

where $T_N(b)$ is the partonic overlap function between two nucleons at impact parameter b. In order to account for the shadowing of the parton density within a nucleus, we also introduced effective parton structure functions $f_{a/A}(x, p_T^2)$ which include medium corrections [18].

To fix the two correlated parameters p_0 and $\sigma_{\rm soft}$, we have assumed constant values of $p_0 = 2$ GeV/c and $\sigma_{\rm soft} = 57$ mb. The resultant total, elastic, and inelastic cross sections agree very well with the experiments from ISR to Tevatron and cosmic-ray energies [22]. We want to emphasize here that the infrared cutoff p_0 in the primary parton-parton scatterings is a phenomenological parameter and is constrained by the experimental values of the total nucleon-nucleon cross section. (As we will discuss below, this infrared singularity of parton cross sections in a dense partonic medium can be regulated naturally by the color screening mass.)

Because of the high gluon density at small x and the large gluon-gluon cross section, the initially produced partons are predominantly gluons. It is very important for the following discussion of the emergence of momentum isotropy that the p_T distributions of the initially produced gluons be almost exponential. The results of the HIJING calculation at RHIC and the CERN Large Hadron Collider (LHC) energies are given in Ref. [14], where the rapidity width of the central plateau Y, the total number of the produced gluons N_G, and their average transverse momentum $\langle k_T \rangle$ are listed. Before we estimate the initial parton number and energy densities, we next have to address the problem of thermalization.

III. THERMALIZATION

We can apply rate equations and particle distribution functions to describe the system only, when approximate local isotropy in momentum space is achieved. At the onset of expansion, scattered partons with very different rapidities are confined to a highly compressed slab. The width $\Delta \approx 2/p_0 = 0.2$ fm of this slab is determined by the virtuality of the scattering partons, which in turn is connected with the transverse momentum cutoff p_0 for perturbative parton scattering.

At this point we adopt a realistic ansatz for the phase-space distribution of the scattered gluonic partons. Following Ref. [14], we define the momentum distribution function as

$$f(\mathbf{k}) = \frac{1}{d_G |\mathbf{k}|} g(\mathbf{k}_T, y), \quad (3)$$

where $\mathbf{k}_T$ and y are the transverse momentum and the rapidity of the gluons, respectively, and $d_G = 16$ is the color-spin degeneracy factor for gluons. Parametrizing the HIJING results $g(\mathbf{k}_T, y)$ can be represented by

$$g(\mathbf{k}_T, y) = \frac{1}{2Y} \left[\Theta(y + Y) - \Theta(y - Y)\right] \tilde{g}(k_T), \quad (4)$$

where the function $\tilde{g}(k_T)$ is explicitly given in Ref. [14] for Au + Au collisions at RHIC and LHC energies. For the spatial part of the distribution function, we assume that the partons form a homogeneous cylinder of length Δ and radius R. The phase-space distribution function then factorizes:

$$F(\mathbf{k}, \mathbf{x}) = f(\mathbf{k}) D(\mathbf{x}), \quad (5)$$

with $D(\mathbf{x})$ given by

$$D(\mathbf{x}) = \frac{1}{\pi R^2 \Delta} \Theta\left(\frac{\Delta^2}{4} - z^2\right) \Theta(R - r). \quad (6)$$

The overall normalization

$$N_G = \int d^3k \int d^3x \; F(\mathbf{k},\mathbf{x}) = \int d^3k \; f(\mathbf{k}) \qquad (7)$$

yields gluon rapidity densities $N_G/2Y = 190$ for RHIC and $N_G/2Y = 600$ for LHC energies.

By local isotropy in momentum space we mean that a parton located in the central region of the collision is surrounded by partons with different but isotropically distributed momenta. This parton does not interact with all the partons in the plasma, but only with those within a distance approximately equal to the parton mean free path. We can imagine a little box in the central region the size of the mean free path Λ_f. The momentum of each particle in the box has components longitudinal and transverse to the beam, k_L and $\mathbf{k}_T$, respectively. We say that local isotropy in momentum space is established when the variance σ_L of the longitudinal momentum distribution of partons in the box equals that of the transverse momentum distribution σ_T. In the case of an exponential distribution we call the isotropic parton system (approximately) thermalized. The variance σ_T is defined as

$$\sigma_T^2 = \frac{1}{2}\langle \mathbf{k}_T^2 \rangle = \frac{1}{2N_G} \int d^3k \; \mathbf{k}_T^2 f(\mathbf{k}) \,. \qquad (8)$$

At RHIC energy we find $\sigma_T = 1.07$ GeV/c using the phase-space distribution of Ref. [14]; the value at LHC energy is 1.76 GeV/c. For the mean free path Λ_f of this initial phase we take [23]

$$\Lambda_f^{-1} = \tfrac{3}{2}\alpha_s \sigma_T, \qquad (9)$$

corresponding to $\Lambda_f = 0.4$ fm (RHIC) and $\Lambda_f = 0.25$ fm (LHC), assuming $\alpha_s = 0.3$.

As the system expands, mainly in the longitudinal direction, partons with longitudinal momentum will leave the central region and σ_L will decrease as a function of time. Assuming that the system evolves approximately by free streaming, the longitudinal position of a parton depends on its rapidity and time,

$$z(t) = z(0) + \tanh(y)t.$$

Here t denotes time in the c.m. system and $z(0)$ is the initial position of the parton along the beam axis [$|z(0)| \leq \frac{\Delta}{2}$]. The phase space distribution $F(\mathbf{k},\mathbf{x})$ depends accordingly on time,

$$F(\mathbf{k},\mathbf{x};t) = F(\mathbf{k},\mathbf{x} - \tanh(y)t\hat{\mathbf{z}}\,;0), \qquad (10)$$

where $\hat{\mathbf{z}}$ is a unit vector along the z direction. Now we can determine σ_L and σ_T as functions of time:

$$\sigma_L^2(t) = \frac{\int d^3x \int d^3k F(\mathbf{k},\mathbf{x};t) k_L^2}{\int d^3x \int d^3k F(\mathbf{k},\mathbf{x};t)}, \qquad (11)$$

where the x integral is over V_f, the volume of a tube of longitudinal length Λ_f, centered at $z = 0$. We find that $\sigma_L(t)$ equals σ_T for $t_{\rm iso} = 0.31$ fm/c (RHIC) and $t_{\rm iso} = 0.23$ fm/c (LHC). For $t \geq t_{\rm iso}$, there is local isotropy in momentum space and we will describe the system by thermal rate equations from then on.

IV. PARTON CHEMISTRY

As discussed in the previous section, the kinematic separation of partons with different rapidity establishes conditions required for the validity of continuum dynamics after a short time of the order of 0.3 fm/c. At this time the momentum space distribution of partons is roughly isotropic locally and approximately exponential. Since we are here primarily interested in the chemical equilibration of the parton gas, we shall assume that the parton distributions can be approximated by thermal phase-space distributions with nonequilibrium fugacities λ_i:

$$f(k;T,\lambda_i) = \mp \sum_{n=1}^{\infty} (\pm\lambda_i)^n e^{-n\beta u\cdot k} = \lambda_i \left(e^{\beta u\cdot k} \pm \lambda_i\right)^{-1}, \qquad (12)$$

where β is the inverse temperature and u^μ is the four-velocity of the local comoving reference frame. The expression (12) is known as the Jüttner distribution. When the parton fugacities λ_i are much less than unity as may happen during the early evolution of the parton system, we can neglect the quantum corrections in (12) and write the momentum distributions in the factorized form

$$f(k;T,\lambda_i) \approx \lambda_i e^{-\beta u\cdot k}. \qquad (13)$$

However, this introduces errors of the order of 40% when the parton phase-space distributions approach chemical equilibrium. As an example, we show the dependence of the screening length μ_D^{-1} for static color-electric fields related to the square of the Debye mass [14],

$$\mu_D^2 = \frac{6g^2}{\pi^2} \int_0^\infty k f(k) dk, \qquad (14)$$

on the gluon fugacity λ_g in Fig. 1. The solid line is the exact perturbative result for the Jüttner distribution (12), the dotted line shows the Boltzmann approximation (13), and the dashed line shows the result obtained for the factorized Bose distribution

$$f(k;T,\lambda_i) = \lambda_i \left(e^{\beta u\cdot k} \pm 1\right)^{-1}. \qquad (15)$$

The dimensionless quantity $\mu_D^2/\lambda_g g^2 T^2$ drops from unity at $\lambda_g = 1$ to $6/\pi^2$ at $\lambda_g = 0$. As can be seen the Boltzmann distribution function (13) is a good approximation to the gluon phase-space density at small $\lambda_g \approx 0$ values. For $\lambda_g \approx 1$ values, however, the approximation (15) applies, which we will adopt in most of the following calculations. Similar, although smaller, violations of factorization occur in the gluon and quark densities and in the various reaction rates.

In general, chemical rections among partons can be quite complicated because of the possibility of initial- and final-state gluon radiation. Multiple radiative emission processes have been investigated in the framework of numerical simulations of parton cascades [1,5]. However, since radiation processes are considerably suppressed in a dense parton medium due to rescattering [15], we shall

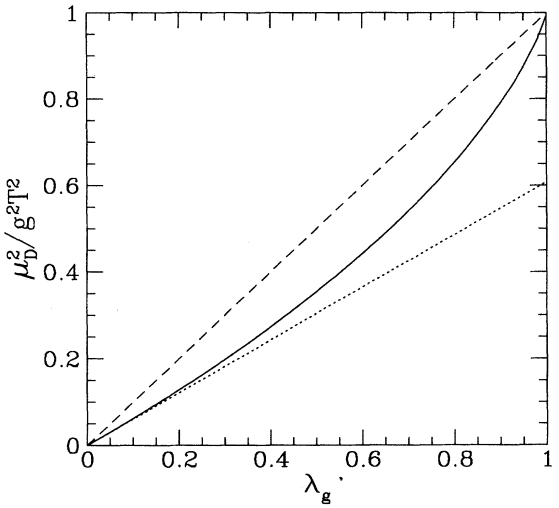

FIG. 1. The square of the thermal screening mass μ_D of color-electric fields scaled by the equilibrium value g^2T^2 is depicted as function of the gluon fugacity λ_g. The solid curve shows the correct result for the Jüttner distribution (12), and the dashed line corresponds to the factorized Bose distribution (15), while the dotted line indicates the Boltzmann approximation (13) applying in the limit of a very dilute gluon plasma.

here consider only processes where a single additional gluon is radiated, such as $gg \to ggg$. In order to permit an approach to chemical equilibrium, the reverse process, i.e., gluon absorption, has to be included as well, which is easily achieved making use of detailed balance. Closer inspection shows that gluon radiation is dominated by the process $gg \to ggg$, because radiative processes involving quarks have substantially smaller cross sections in perturbative QCD, and quarks are considerably less abundant than gluons in the initial phase of the chemical evolution of the parton gas. Here we are interested in understanding the basic mechanisms underlying the formation of a chemically equilibrated quark-gluon plasma, and the essential time scales. We hence restrict our considerations to the dominant reaction mechanisms for the equilibration of each parton flavor. These are just four processes [24]

$$gg \leftrightarrow ggg, \quad gg \leftrightarrow q\bar{q}. \tag{16}$$

Other scattering processes ensure the maintenance of thermal equilibrium ($gg \leftrightarrow gg$, $gq \leftrightarrow gq$, etc.) or yield corrections to the dominant reaction rates ($gq \leftrightarrow qgg$, etc.).

Restricting ourselves to the reactions (16) and assuming that elastic parton scattering is sufficiently rapid to maintain local thermal equilibrium, the evolution of the parton densities is governed by the master equations

$$\partial_\mu(n_g u^\mu) = n_g(R_{2\to3} - R_{3\to2}) - (n_g R_{g\to q} - n_q R_{q\to g}) , \tag{17}$$

$$\partial_\mu(n_q u^\mu) = \partial_\mu(n_{\bar{q}} u^\mu) = n_g R_{g\to q} - n_q R_{q\to g}, \tag{18}$$

where $R_{2\to3}$ and $R_{3\to2}$ denote the rates for the process $gg \to ggg$ and its reverse, and $R_{g\to q}$ and $R_{q\to g}$ those for the process $gg \to q\bar{q}$ and its reverse, respectively. The temperature evolves according to the hydrodynamic equation

$$\partial_\mu(\varepsilon u^\mu) + P\,\partial_\mu u^\mu = 0, \tag{19}$$

where viscosity effects have been neglected [25].

The rates depend on the temperature and the fugacities in a rather complicated way. In order to make analytical progress, we here assume factorization of the dependence of the densities on the fugacities, i.e., Eq. (15), and postpone a full numerical evaluation of the rate equations. The rates can then be factorized in the following simple way:

$$n_g\,(R_{2\to3} - R_{3\to2}) = \frac{1}{2}\sigma_3\, n_g^2 \left(1 - \frac{n_g}{\tilde{n}_g}\right), \tag{20}$$

$$n_g R_{g\to q} - n_q R_{q\to g} = \frac{1}{2}\sigma_2 n_g^2 \left(1 - \frac{n_q n_{\bar{q}} \tilde{n}_g^2}{\tilde{n}_q \tilde{n}_{\bar{q}} n_g^2}\right) , \tag{21}$$

where σ_3 and σ_2 are thermally averaged, velocity weighted cross sections,

$$\sigma_3 = \langle \sigma(gg \to ggg) v \rangle, \quad \sigma_2 = \langle \sigma(gg \to q\bar{q}) v \rangle , \tag{22}$$

and $\tilde{n}_i$ denote the densities for $\lambda_i = 1$. Equations (17,18) can then be rewritten as

$$\partial_\mu(\lambda_g \tilde{n}_g u^\mu) \approx \tilde{n}_g R_3 \lambda_g(1 - \lambda_g) - 2\tilde{n}_g R_2 \lambda_g \left(1 - \frac{\lambda_q \lambda_{\bar{q}}}{\lambda_g^2}\right), \tag{23}$$

$$\partial_\mu(\lambda_q \tilde{n}_q u^\mu) = \partial_\mu(\lambda_{\bar{q}} \tilde{n}_{\bar{q}} u^\mu) \approx \tilde{n}_g R_2 \lambda_g \left(1 - \frac{\lambda_q \lambda_{\bar{q}}}{\lambda_g^2}\right), \tag{24}$$

where the density weighted reaction rates R_3 and R_2 are defined as

$$R_3 = \tfrac{1}{2}\sigma_3 n_g, \quad R_2 = \tfrac{1}{2}\sigma_2 n_g. \tag{25}$$

In order to obtain simple solutions to Eqs. (23,24) we will assume that the expansion of the parton fireball is purely longitudinal, yielding Bjorken's scaling solution [26] of the hydrodynamic equation (19):

$$\frac{d\varepsilon}{d\tau} + \frac{\varepsilon + P}{\tau} = 0, \tag{26}$$

where τ is the proper time. This assumption is expected to be very well satisfied during the early expansion phase of the fireball, especially at proper time $\tau \ll R_A$, where R_A is the transverse radius of the fireball. Further assuming the ultrarelativistic equation of state

$$\varepsilon = 3P = [a_2 \lambda_g + b_2(\lambda_q + \lambda_{\bar{q}})]\; T^4, \tag{27}$$

with $a_2 = 8\pi^2/15$, $b_2 = 7\pi^2 N_f/40$, where N_f is the number of dynamical quark flavors, we obtain from (26) a relation between the proper-time dependence of the temperature and the fugacities. Denoting the derivative with respect to τ by an overdot, we find

$$\frac{\dot{\lambda}_g + b(\dot{\lambda}_q + \dot{\lambda}_{\bar{q}})}{\lambda_g + b(\lambda_q + \lambda_{\bar{q}})} + 4\frac{\dot{T}}{T} + \frac{4}{3\tau} = 0, \tag{28}$$

where

$$b = b_2/a_2 = 21N_f/64. \tag{29}$$

Equation (28) is easily integrated, resulting in

$$[\lambda_g + b(\lambda_q + \lambda_{\bar{q}})]^{3/4} T^3 \tau = \text{const.} \tag{30}$$

For a fully equilibrated quark-gluon plasma ($\lambda_g = \lambda_q = \lambda_{\bar{q}} = 1$) this corresponds to the Bjorken solution $T(\tau) = T_0(\tau_0/\tau)^{1/3}$.

In the same approximation, i.e., neglecting interactions and using the factorized distributions, the gluon and quark equilibrium densities are related to the temperature parameter T by

$$\tilde{n}_g = \frac{16}{\pi^2}\zeta(3)T^3 \equiv a_1 T^3, \tag{31}$$

$$\tilde{n}_q = \frac{9}{2\pi^2}\zeta(3)N_f T^3 \equiv b_1 T^3. \tag{32}$$

We can also rewrite Eqs. (19,23,24) as equations determining the time dependence of the parameters T, λ_g, and λ_q. In the longitudinal scaling expansion we find

$$\partial_\mu(n_g u^\mu) = u^\mu \partial_\mu n_g + n_g \partial_\mu u^\mu = \frac{\partial n_g}{\partial \tau} + \frac{n_g}{\tau}. \tag{33}$$

After division by n_g and n_q, respectively, the rate equations take the form

$$\frac{\dot{\lambda}_g}{\lambda_g} + 3\frac{\dot{T}}{T} + \frac{1}{\tau} = R_3(1-\lambda_g) - 2R_2\left(1 - \frac{\lambda_q\lambda_{\bar{q}}}{\lambda_g^2}\right), \tag{34}$$

$$\frac{\dot{\lambda}_q}{\lambda_q} + 3\frac{\dot{T}}{T} + \frac{1}{\tau} = R_2\frac{a_1}{b_1}\left(\frac{\lambda_g}{\lambda_q} - \frac{\lambda_{\bar{q}}}{\lambda_g}\right), \tag{35}$$

with the additional constraint

$$(\lambda_q - \lambda_{\bar{q}})T^3\tau = \text{const} \tag{36}$$

expressing baryon number conservation. Being interested in parton thermalization at very high collision energies, we shall assume baryon symmetric matter, i.e., $\lambda_q = \lambda_{\bar{q}}$, which solves (36) trivially. Equations (30,34,35) determine the evolution of $T(\tau), \lambda_g(\tau)$, and $\lambda_q(\tau)$ towards chemical equilibrium, once the reaction rates R_2 and R_3 are known. We now turn to these.

V. THE EQUILIBRATION RATES

The cross sections σ_2 and σ_3 contain infrared singularities if calculated in naive perturbation theory. Recently, Braaten and Pisarski [27] proposed an effective perturbation theory, based on a resummation of subsets of diagrams (hard thermal loops), which takes screening effects into account and avoids inconsistencies of the naive perturbation theory at finite temperature. This method results in using effective propagators and vertices, which show a complicated momentum dependence. It has been used, e.g., to calculate the stopping power [28] and the viscosity [29] of the quark-gluon plasma, which also follow both from elastic parton collisions. In order to calculate σ_2 and σ_3 we will adopt a simplified version of this idea by introducing momentum-independent screening masses into the propagators, whenever infrared divergences arise otherwise. In the case of the stopping power and the viscosity this approximation provides quantitatively good results.

A. Gluon equilibration

The rate R_3 for the process $gg \to ggg$ depends on the triple differential radiative gluon-gluon cross section, which can be written as [30]

$$\frac{d\sigma^{2\to3}}{d^2q_\perp dy d^2k_\perp} \approx \frac{d\sigma^{2\to2}}{d^2q_\perp}\left[\frac{C_A\alpha_s}{\pi^2}\frac{q_\perp^2}{k_\perp^2(\mathbf{k}_\perp - \mathbf{q}_\perp)^2}\right], \tag{37}$$

where $C_A = 3$ is the Casimir operator of the adjoint representation of SU(3). Here $\mathbf{k}_\perp$ denotes the transverse momentum and y the longitudinal rapidity of the radiated gluon, and $\mathbf{q}_\perp$ denotes the momentum transfer in the elastic collision. The in-medium cross section for elastic scattering of two gluons [31],

$$\frac{d\sigma^{2\to2}}{d^2q_\perp} = C_{gg}\frac{2\alpha_s^2}{(q_\perp^2 + \mu_D^2)^2}, \tag{38}$$

with $C_{gg} = \frac{9}{4}$, is screened by the Debye mass.

In the presence of a dense medium the emission of radiation is suppressed, if the gluons scatter again before the emission is completed (Landau-Pomeranchuk effect), leading to the condition [32]

$$k_\perp \Lambda_f > 2\cosh y, \tag{39}$$

where Λ_f is the mean free path of a gluon. The contribution from soft radiation is strongly suppressed by this effect.

To obtain the gluon production rate R_3 we must integrate the differential cross section (37) over momentum transfer $\mathbf{q}_\perp$ and the phase space of the radiated gluon. The integrand is singular at $\mathbf{k}_\perp = \mathbf{q}_\perp$. We shall deal with this problem in two different ways. First, we shall assume that $\mathbf{k}_\perp \cdot \mathbf{q}_\perp = 0$ in the integrand, i.e., that the radiation is mostly perpendicular to the reaction plane. Later we will average over the angle between $\mathbf{k}_\perp$ and $\mathbf{q}_\perp$, introducing an infrared cutoff to avoid the singularity. In the first approach, we replace $(\mathbf{k}_\perp - \mathbf{q}_\perp)^2$ by $(k_\perp^2 + q_\perp^2)$ in the integrand, effectively suppressing collinear bremsstrahlung. We then arrive at the following modified differential cross section:

$$\frac{d\sigma^{2\to3}}{dq_\perp^2\,dy dk_\perp^2} \approx \frac{2C_A C_{gg}\alpha_s^3 q_\perp^2}{(q_\perp^2+\mu_D^2)^2 k_\perp^2 (k_\perp^2+q_\perp^2)}\,\theta(k_\perp\Lambda_f - 2\cosh y)\theta(\sqrt{s}-k_\perp\cosh y), \tag{40}$$

where the step functions account for the Landau-Pomeranchuk effect (39) and for energy conservation. $\langle s\rangle = 18T^2$ is the average squared center-of-mass energy of two gluons in the thermal gas. The integrated elastic gluon-gluon cross section in the medium is, from Eq. (38),

$$\sigma^{2\to2} = 2\pi C_{gg}\frac{\alpha_s^2}{\mu_D^2}, \tag{41}$$

yielding a fugacity independent mean free path

$$\Lambda_f^{-1} = \sigma^{2\to2} n_g = \tfrac{9}{8} a_1 \alpha_s T. \tag{42}$$

Using these values we evaluate the chemical gluon equilibration rate $R_3 = \frac{1}{2} n_g \sigma_3$, as defined in Eq. (24), numerically. This rate scales with the temperature linearly but is a complicated function of the gluon fugacity. The solid line in Fig. 2 shows the scaled rate R_3/T versus λ_g for a coupling constant $\alpha_s = 0.3$. The dotted line corresponds to the analytical fit

$$R_3 = 2.1\alpha_s^2 T\left(2\lambda_g - \lambda_g^2\right)^{1/2}, \tag{43}$$

which will be used in solving the time-dependent rate equations discussed in the next section.

We have also studied another solution to the problem posed by the collinear singularity in Eq. (37), namely, to add a screening mass to $(\mathbf{k}_\perp - \mathbf{q}_\perp)^2$. The integral over the relative angle φ between $\mathbf{k}_\perp$ and $\mathbf{q}_\perp$ can then be performed analytically, yielding

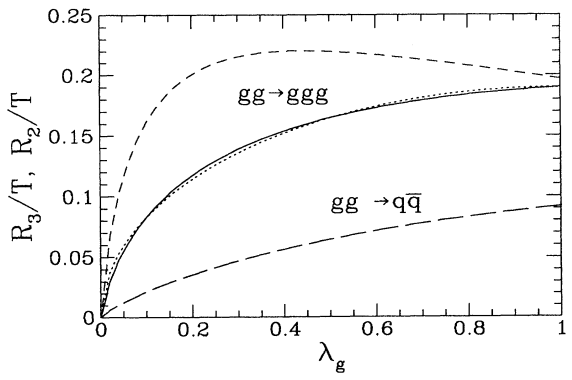

FIG. 2. The scaled gluon production rate R_3/T is shown as function of the gluon fugacity λ_g for $\alpha_s = 0.3$. The solid line shows the numerical result, using the approximation (42), while the dotted line shows the analytical fit (45). The dashed line represents the result obtained with the screening approximation (46) to the collinear singularity in the bremsstrahlung cross section. The long-dashed curve shows the scaled quark production rate R_2/T for 2.5 quark flavors.

$$\frac{1}{2\pi}\int d\varphi[(\mathbf{k}_\perp - \mathbf{q}_\perp)^2 + \mu^2]^{-1} = [(k_\perp^2 + q_\perp^2 + \mu^2)^2 - 4k_\perp^2 q_\perp^2]^{-1/2}. \tag{44}$$

The rate R_3 obtained in this way for $\mu = \mu_D$ is shown in Fig. 2 by the dashed line. It is somewhat larger than the rate obtained by setting $\cos\varphi = 0$, so that (43) can be considered as a conservative estimate.

We finally note that the process $gg \to ggg$, which drives the chemical equilibration of the gluon plasma, has recently been considered by Enqvist and Sirkka [33], who showed that it is sufficiently suppressed to avoid equilibration of the QCD plasma in the very early Universe. For temperatures in excess of 10^{14} GeV the equilibration of gluons proceeds more slowly than the cosmic expansion.

B. Quark equilibration

The total cross section for the process $gg \to q\bar{q}$ is dominated by the Compton diagrams involving exchange of a virtual light quark in the t or u channel. For massless quarks the differential cross section [31]

$$\frac{d\sigma_q}{dt} = \frac{\pi\alpha_s^2}{s^2}\left[\frac{1}{6}\left(\frac{u}{t}+\frac{t}{u}\right) - \frac{3}{8} + \frac{3ut}{4s^2}\right] \tag{45}$$

diverges as $u, t \to 0$; hence the medium-induced effective quark mass plays a crucial role. Unfortunately, a complete calculation of the cross section for the process $gg \to q\bar{q}$ within the framework of thermal field theory with hard thermal loop resummation [27] has not yet been done. But since the divergence of the cross section is only logarithmic in this case, it may be a sufficiently good estimate to simply substitute the effective thermal quark mass as cutoff in the divergent integral over momentum transfer. The thermal quark mass, using Bose and Fermi equilibrium distributions, is [34]

$$M^2 = \left(\lambda_g + \frac{1}{2}\lambda_q\right)\frac{4\pi}{9}\alpha_s T^2, \tag{46}$$

yielding the total cross section (for $s \gg M^2$):

$$\sigma_q \approx \frac{\pi\alpha_s^2}{3s}\left(\ln\frac{s}{M^2} - \frac{7}{4}\right). \tag{47}$$

Integrating over thermal gluon distributions and inserting the average thermal $\langle s\rangle = 18T^2$ in the logarithm, we have

$$\sigma_2 \approx N_f\langle\sigma_q v\rangle \approx N_f\frac{\pi\alpha_s^2}{24T^2}\left(\frac{\zeta(2)}{\zeta(3)}\right)^2\left(\ln\frac{81}{\pi\alpha_s(\lambda_g+\frac{1}{2}\lambda_q)} - \frac{11}{4}\right). \tag{48}$$

Neglecting λ_q in the logarithm, we obtain the light quark production rate

$$R_2 = \tfrac{1}{2}\sigma_2 n_g \approx 0.24 N_f\, \alpha_s^2 \lambda_g T \ln(1.65/\alpha_s\lambda_g). \quad (49)$$

The long-dashed line in Fig. 2 shows the normalized rate R_2/T for $N_f = 2.5$, taking into account the reduced phase space of strange quarks at moderate temperatures, as function of the gluon fugacity.

The quark equilibration rate has recently been investigated by Altherr and Seibert [35] in a more complete treatment of finite temperature QCD, taking into account effective propagators for gluons and quarks. Their result

$$R_2 = \frac{16}{27\pi}\alpha_s^2 T(\ln \alpha_s^{-1})^2, \quad (50)$$

valid only for $\lambda_g = 1$, agrees roughly with our estimate (49) for values of α_s that are not much larger than 0.3.

VI. RESULTS

A. Initial conditions

We have solved the rate equations (34,35) and the energy conservation equation (28) simultaneously by numerical integration using a fourth order Runge-Kutta method. The initial conditions for these rate equations are the number density $n_0 = n(t_{\rm iso})$ and the transverse energy density $\varepsilon_T = \varepsilon_T(t_{\rm iso})$ of gluonic partons, where

$$n_0 = \frac{1}{\pi R^2 t_{\rm iso}}\frac{N_G}{2Y}, \quad \varepsilon_T = n_0\langle k_T\rangle. \quad (51)$$

The total initial gluon energy density is $\varepsilon_0 = 4\varepsilon_T/\pi$. We obtain $n_0 = 4.2$ fm^{-3} and $\varepsilon_0 = 6.4$ GeV/fm^3 at RHIC energy, and $n_0 = 17$ fm^{-3} and $\varepsilon_0 = 38$ GeV/fm^3 at LHC energy. Quarks contribute a smaller amount to the initial parton energy density, because the quark-producing cross sections are smaller in perturbative QCD than those for gluon production [36]. The total quark contribution to the energy density we estimate as 30%, yielding total initial energy densities of 8.5 GeV/fm^3 at RHIC and 60 GeV/fm^3 at LHC.

The temperature and fugacities at the beginning of hydrodynamical evolution ($t = t_{\rm iso}$) are obtained assuming a thermal, but not chemically equilibrated Bose distribution for gluons, i.e.,

$$n_0 = \lambda_g^0 a_1 T_0^3, \quad \varepsilon_0 = \lambda_g^0 a_2 T_0^4\ , \quad (52)$$

where $a_1 \approx 1.95$, $a_2 \approx 5.26$. The quark fugacity is taken as $\lambda_q^0 = \lambda_g^0/5$, corresponding to a ratio 3:1 of the initial gluon number to the combined number of quarks and antiquarks. Table I shows these relevant quantities at the moment $t_{\rm iso}$, for Au + Au collisions at RHIC and LHC energies.

We should emphasize that the initial conditions used here result from the HIJING model calculation in which only initial direct parton scatterings are taken into account. Because of the fact that HIJING is a QCD motivated phenomenological model, there are some uncertainties related to the initial parton production.

TABLE I. Values of the relevant parameters characterizing the parton plasma at the moment $t_{\rm iso}$, when local isotropy of the momentum distribution is first reached.

	RHIC	LHC
$t_{\rm iso}$ (fm/c)	0.31	0.23
ε_0 (GeV/fm^3)	6.4	38
n_0 (fm^{-3})	4.2	17
$\varepsilon_{\rm tot}$ (GeV/fm^3)	8.5	60
Λ_f (fm)	0.40	0.24
$\langle k_T\rangle$ (GeV)	1.17	1.76
T_0 (GeV)	0.57	0.83
λ_g^0	0.09	0.14
λ_q^0	0.02	0.03

(1) As we mentioned in Secs. I and II, the minijet cross section and thus the initial number of scattered partons depend on the p_T cutoff p_0. This cutoff and the corresponding soft inclusive cross section $\sigma_{\rm soft}$ are constrained by the energy dependence of the total pp and $p\bar{p}$ cross sections. Even though one may introduce other physical arguments to derive values of p_0 and $\sigma_{\rm soft}$ [21], the two parameters cannot be determined uniquely from the phenomenology of currently measured observables. This puts a considerable uncertainty on the total number of primary parton-parton collisions. Changing p_0 from 2 to 1.5 GeV/c, as in the original simulations of the parton cascade model [5], increases our initial parton number by about a factor of 3 at RHIC energy. We explore this more optimistic scenario briefly below.

(2) Since most of partons produced are gluons, their number is sensitive to the gluon structure function $f_g(x)$ at small x. But so far there is still no precise measurement of the gluon structure function in the small x region where most of the minijets originate at RHIC energy. Furthermore, we have no handle experimentally so far on the nuclear shadowing of the gluon structure function. In HIJING we have assumed the same shadowing for gluons and quarks which has reduced the parton production by half inside a heavy nucleus [22].

To pin these uncertainties down, the measurement of two-particle correlation functions in azimuthal angle in the transverse plane has been proposed [37] to further constrain p_0 and $\sigma_{\rm soft}$, and a systematical measurement of pp, pA, and AA interactions has to be made [38] to study the gluon shadowing. We note that changes in p_0 and the nuclear shadowing are correlated, because a decrease of p_0 will increase shadowing.

(3) In the Monte Carlo simulation of the parton cascade model [1], besides the secondary parton interactions considered here, primary-secondary collisions are also taken into account. In these processes, the produced partons interact again with the incoming partons from the projectile or target producing more partons that cannot be clearly identified as being of truly primary or secondary origin. Interactions between primary and secondary partons are suppressed by formation time effects, because those partons inside the nuclei, which have not

interacted, have already passed through the interaction region and thus do not contribute to secondary parton scatterings. These effects have been investigated in the framework of the parton cascade, but there is some uncertainty at present whether they can reduce the abundance of primary-secondary scatterings significantly [5,39]. The number of scattered partons in the parton cascade model is also enhanced by the inclusion of soft interactions, which are not described by perturbative QCD processes and hence have no place in the present discussion. We remark on string interactions with the parton plasma briefly at the end of the following subsection.

B. Evolution of the parton plasma

The evolution of the temperature and the fugacities are shown in Fig. 3. We find that the parton gas cools considerably faster than predicted by Bjorken's scaling solution ($T^3\tau = \text{const}$), because the production of additional partons aproaching the chemical equilibrium state consumes an appreciable amount of energy. This can be also deduced from Eq. (30): While the fugacities increase, the product $T^3\tau$ must decrease.

The accelerated cooling, on the other hand, impedes the chemical equilibration process, which is more apparent at RHIC [Fig. 3(a)] than at LHC energies [Fig. 3(b)]. In order to see where the perturbative description of the parton plasma is applicable we investigate the time evolution of the total energy density, Eq. (25). The solid lines in Fig. 4 correspond to the initial conditions shown in Table I, while the dashed line corresponds to the more optimistic estimate of the initial gluon production at RHIC. One realizes that the perturbative parton plasma has a lifetime of 1–2 fm/c at RHIC, while at LHC the plasma may exist in a deconfined phase as long as 5–6 fm/c. The evolution of the energy density is remarkably insensitive to the magnitude of the gluon equilibration rate R_3. A change in R_3 by a factor of 2 is hardly noticeable in the function $\varepsilon(\tau)$.

The initial conditions obtained in Sec. III depend sensitively on the low-momentum cutoff p_0 used to regularize the minijet cross sections. As mentioned in the previous subsection, ambiguities in the determination of p_0 allow for a range of 1.5–2 GeV in the low-momentum cutoff at RHIC energy. Using the smaller value [5,40] one obtains an initial gluon fugacity $\lambda_g \approx 0.27$, which is 3 times larger than the value discussed above. Using this value we find a larger initial energy density and hence a longer lifetime of 3.5 fm/c for the parton plasma at RHIC (see the dashed curve in Fig. 4). A higher value of λ_g at $t_{\rm iso}$ can also result from rescattering of gluons during the "free-streaming" period between the end of initial semihard scattering and $t_{\rm iso}$. Indeed, the parton cascade simulations [5] indicate a rapid increase of gluon density during this prethermal phase. We conclude that the validity of this scenario of quark-gluon plasma production by perturbative parton scattering is uncertain at RHIC energies, but very likely in the LHC energy domain.

From our investigation emerges the following scenario of a nuclear collision at collider energies: Within 0.2–0.3 fm/c a dense parton gas is produced at central rapidities, which can be described as a locally thermalized, but not chemically equilibrated quark-gluon pasma. In the fragmentation region, where the parton gas created by minijets is not sufficiently dense to screen color fields, strings and color ropes are formed [41,42], which decay by nonperturbative QCD processes on a time scale of about 1 fm/c. These strings extend between the wounded nuclei and the surface of the parton plasma, penetrating up to a screening length determined by the actual Debye mass.

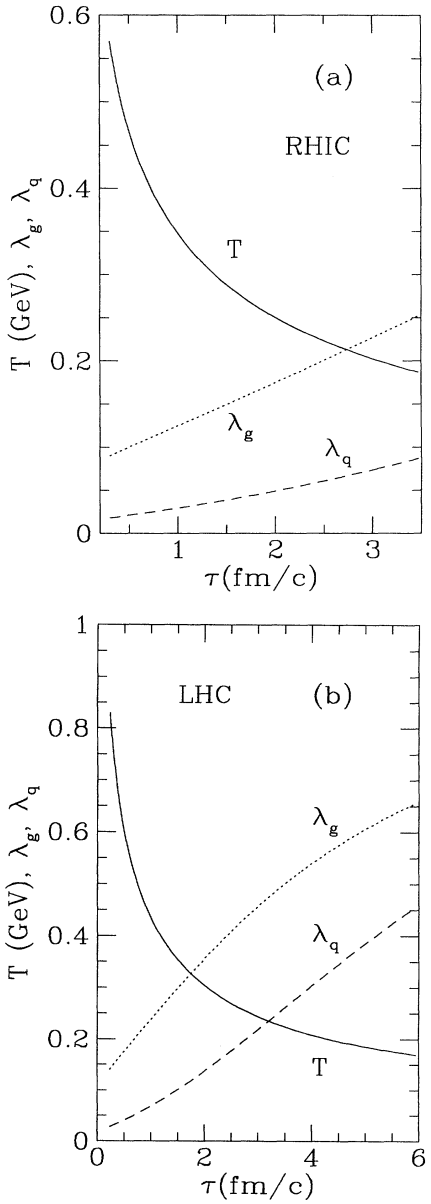

FIG. 3. Time evolution of the temperature T and the fugacities λ_g and λ_q of gluons and quarks in the parton plasma created in Au + Au collisions at (a) the RHIC c.m. energy of 100 GeV/nucleon, (b) the LHC c.m. energy of 3000 GeV/nucleon. The initial values for T, λ_g, and λ_q are determined from simulations with the HIJING code and are listed in Table I.

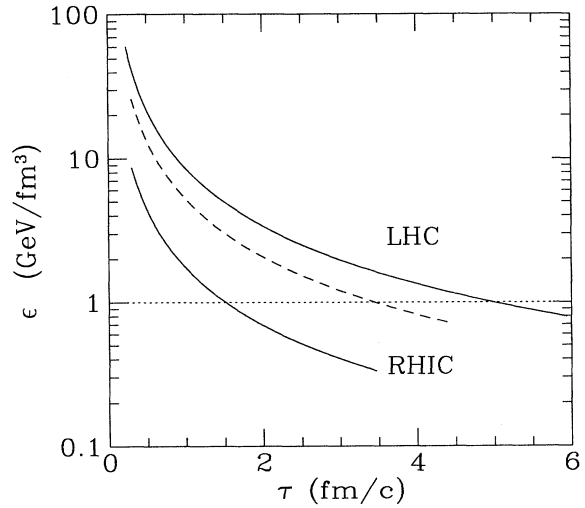

FIG. 4. Time dependence of the energy density of the parton plasma at RHIC and LHC energies. The solid lines show the results obtained with the initial values taken from Table I. The dashed line shows the effect of a 3 times higher initial gluon density at RHIC energy, corresponding to QCD cutoff $p_0 \approx 1.5$ GeV instead of $p_0 = 2$ GeV. Whereas a well-developed parton plasma is predicted to be formed at the LHC, the prediction for RHIC is uncertain.

As in the Bjorken scenario, the scaling expansion of the system can best be described by using the proper time τ and space-time rapidity

$$\eta = \tfrac{1}{2} \ln \frac{t + x}{t - x} \tag{53}$$

variables. This scenario is schematically shown in Fig. 5, where the different space-time regions of the prethermal creation phase, the parton plasma, and the string-dominated phase are indicated.

The main difference to the conventional Bjorken scenario [26] is the far shorter formation time in the central rapidity region, corresponding to a much higher initial temperature. The Bjorken scenario, however, most probably applies to the fragmentation region, where the nonperturbative color ropes may also decay into a quark-gluon plasma. At the interface between the two regions a reheating of the parton plasma may occur by dissipation of field energy stored in the strings. The dissipation of field energy in a quark-gluon plasma was recently studied by Eskola and Gyulassy [43]. At RHIC energies, where the approach discussed here leads to a rather low initial density of partons, color flux tubes may still permeate the whole central region. This would result in multiple interactions between partons from minijet cascades and the soft component modeled by color strings or ropes. In addition, the temperature falls so rapidly that it is difficult to maintain thermal equilibrium by elastic two-body collisions among partons. At RHIC energies the characteristic collision rate, given by the inverse mean free path Λ_f^{-1}, is comparable to the cooling rate $\dot{T}/T$. As discussed by the authors of Ref. [43], such a state would exhibit large viscosity effects which can substantially slow down the cooling rate of the QCD plasma.

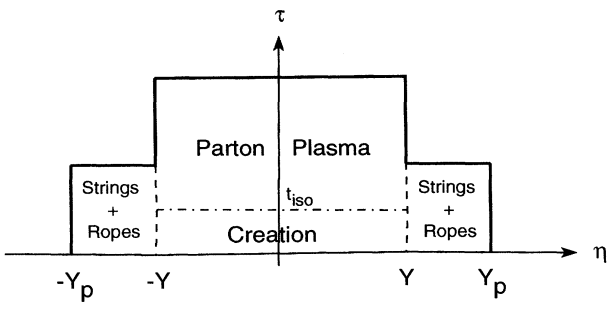

FIG. 5. Schematic space-time diagram of the evolution of QCD matter in the initial phase of an ultrarelativistic heavy ion collision. The central rapidity region is dominated by a thermalized, but not chemically equilibrated parton plasma after $t_{iso} \approx 0.2$–0.3 fm/c.

VII. CONCLUSIONS

Our results support the picture emerging from numerical simulations of parton cascades and simple estimates that the highly excited parton plasma created in ultrarelativistic nuclear collisions is initially mainly a gluon plasma. Our results have important implications for several experimental signals associated with quark-gluon plasma formation, as has been pointed out before [8–11,44,45]: Rapid gluon thermalization at a high initial temperature leads to a substantial thermal contribution to the total yield of charmed quarks. This increase comes on top of a substantial suppression of primary charm production by nuclear shadowing of gluon distributions in the central rapidity region. Hence the unambiguous observation of this charm enhancement will require the comparative study of $p + p$, $p + A$, and $A + A$ collisions at the same center-of-mass energy.

The lack of chemical equilibration in the quark and gluon densities, on the other hand, causes a severe depletion of the number of emitted lepton pairs compared with the naive thermal estimate. However, the shift towards higher invariant masses of the steeply falling lepton-pair spectrum due to the larger initial temperature in the plasma can conceivably offset this suppression [44,45].

Reliable quantitative predictions for these experimental signatures require complete microscopic simulations of the parton cascade which include the medium modification of cross section and effective masses discussed in this paper. As we have shown, these medium effects slow the chemical equilibration of the parton plasma down. How can the medium dependence of the parton cross sections be included in microscopic simulations? Since these calculations trace the full space-time evolution of parton densities, it would be straightforward to calculate the color screening length, as well as the effective medium-induced masses of collective gluon and quark modes (plasmons and plasminos) as function of time. These quantities could then be used as input parameters for the determination of medium-dependent scattering cross sections and branching rates.

An unresolved issue remains in the medium depen-

dence of the lower cutoff p_0 used to regularize perturbative QCD cross sections, which was fixed at $p_0 = 2$ GeV/c in HIJING and at a similar, but energy-dependent value in the parton cascade. One possible way of approach would be to identify an upper limit to the (medium-dependent) running QCD coupling constant, above which perturbative cross sections cannot be used. This limit α_0 could be chosen such that it equals $\alpha_s(p_0)$ in vacuum; but it would correspond to a different momentum cutoff, or even no cutoff at all, at high parton densities [46].

ACKNOWLEDGMENTS

We would like to thank K. Kinder-Geiger for his careful reading of the manuscript and several helpful discussions on the parton cascade. We are indebted to D. Seibert for pointing out an error in our calculation of the quark equilibration rate. This work was partially supported by the U.S. Department of Energy (DE-FG05-90ER40592) and the N.C. Supercomputing Center.

[1] K. Geiger and B. Müller, Nucl. Phys. **B369**, 600 (1992); K. Geiger, Phys. Rev. D **47**, 133 (1993); D. Boal, Phys. Rev. C **33**, 2206 (1986).
[2] R. Anishetty, P. Köhler, and L. McLerran, Phys. Rev. D **22**, 2793 (1980).
[3] R. C. Hwa and K. Kajantie, Phys. Rev. Lett. **56**, 696 (1986).
[4] J. P. Blaizot and A. H. Mueller, Nucl. Phys. **B289**, 847 (1987).
[5] K. Geiger, Phys. Rev. D **46**, 4965 (1992); **46**, 4986 (1992).
[6] I. Kawrakow, H.-J. Möhring, and J. Ranft, Nucl. Phys. **A544**, 471c (1992).
[7] B. Müller, in *Particle Production in Highly Excited Matter*, edited by H. Gutbrod and J. Rafelski, NATO-ASI Series B (Plenum Press, New York, 1993), Vol. 303, p. 11.
[8] E. Shuryak, Phys. Rev. Lett. **68**, 3270 (1992).
[9] B. Müller and X. N. Wang, Phys. Rev. Lett. **68**, 2437 (1992).
[10] I. Kawrakow and J. Ranft, University of Leipzig Report No. UL-HEP-92-08, 1992; B. Kämpfer and O. P. Pavlenko, Phys. Lett. B **289**, 127 (1992).
[11] K. Geiger and J. I. Kapusta, Phys. Rev. D **47**, 4905 (1993).
[12] See, e.g., G. Baym, H. Monien, C. J. Pethick, and D. G. Ravenhall, Phys. Rev. Lett. **64**, 1867 (1990).
[13] With the possible exception of processes sensitive to static color-magnetic interactions. Such interactions are believed to be screened at momenta below the order of (g^2T). For an attempt to derive a consistent analytical theory of color-magnetic screening, see T. S. Biró and B. Müller, Nucl. Phys. A (to be published).
[14] T. S. Biró, B. Müller, and X. N. Wang, Phys. Lett. B **283**, 171 (1992).
[15] M. Gyulassy and X.-N. Wang, Report No. LBL-32682, 1993.
[16] C. Albajar *et al.*, Nucl. Phys. **B309**, 405 (1988).
[17] K. Kajantie, P. V. Landshoff, and J. Lindfors, Phys. Rev. Lett. **59**, 2527 (1987); K. J. Eskola, K. Kajantie, and J. Lindfors, Nucl. Phys. **B323**, 37 (1989).
[18] X.-N. Wang and M. Gyulassy, Phys. Rev. D **44**, 3501 (1991).
[19] P. Sjöstrand and M. van Zijl, Phys. Rev. D **36**, 2019 (1987).
[20] See, e.g., R. D. Field, *Applications of Perturbative QCD*, Frontiers in Physics Vol. 77 (Addison-Wesley, Redwood City, CA, 1989).
[21] X.-N. Wang, Phys. Rev. D **43**, 104 (1991).
[22] X.-N. Wang and M. Gyulassy, Phys. Rev. D **45**, 844 (1992).
[23] For justification of this choice see Eq. (42). We have set $a_1 \approx 2$ and $T \approx \frac{2}{3}\sigma_T$.
[24] T. Matsui, B. Svetitsky, and L. McLerran, Phys. Rev. D **34**, 783 (1986).
[25] P. Danielewicz and M. Gyulassy, Phys. Rev. D **31**, 53 (1985); A. Hosoya and K. Kajantie, Nucl. Phys. **B250**, 666 (1985); S. Gavin, *ibid.* **A435**, 826 (1985).
[26] J. D. Bjorken, Phys. Rev. D **27**, 140 (1983).
[27] E. Braaten and R. D. Pisarski, Nucl. Phys. **B337**, 569 (1990).
[28] M. H. Thoma and M. Gyulassy, Nucl. Phys. **B351**, 491 (1991); E. Braaten and M. H. Thoma, Phys. Rev. D **44**, 1298 (1991), **44**, 2625 (1991); M. H. Thoma, Phys. Lett. B **273**, 128 (1991).
[29] M. H. Thoma, Phys. Lett. B **269**, 144 (1991).
[30] J. F. Gunion and G. Bertsch, Phys. Rev. D **25**, 746 (1982).
[31] R. Cutler and D. Sivers, Phys. Rev. D **17**, 196 (1978).
[32] M. Gyulassy, M. Plümer, M. H. Thoma, and X.-N. Wang, Nucl. Phys. **A538**, 37c (1992). [Note that the factor of 2 appearing in Eq. (39) is missing in this reference.]
[33] K. Enqvist and J. Sirkka, Report No. NORDITA-93-32-P, 1993.
[34] V. V Klimov, Zh. Eksp. Teor. Fiz. **82**, 336 (1982) [Sov. Phys. JETP **55**, 199 (1982)]; H. A. Weldon, Phys. Rev. D **26**, 2789 (1982).
[35] T. Altherr and D. Seibert, Report No. CERN-TH.6882/93, 1993.
[36] L. V. Gribov, E. M. Levin, and M. G. Ryskin, Phys. Rep. **100**, 1 (1983).
[37] X.-N. Wang, Phys. Rev. D **46**, R1900 (1992); **47**, 2754 (1993).
[38] X.-N. Wang and M. Gyulassy, Phys. Rev. Lett. **68**, 1480 (1992).
[39] K. J. Eskola and X.-N. Wang, Report No. LBL-34156, 1993.
[40] N. Abou-El-Naga, K. Geiger, and B. Müller, J. Phys. G **18**, 797 (1992).
[41] See, e.g., B. Andersson, G. Gustafsson, and T. Sjöstrand, Z. Phys. C **6**, 235 (1980).
[42] T. Biró, H. B. Nielsen, and J. Knoll, Nucl. Phys. **B245**, 449 (1984).
[43] K. J. Eskola and M. Gyulassy, Phys. Rev. C **47**, 2329 (1993).
[44] K. Geiger and J. I. Kapusta, Phys. Rev. Lett. **70**, 1920 (1993).
[45] E. Shuryak and L. Xiong, Phys. Rev. Lett. **70**, 2241 (1993).
[46] This idea was developed in discussions with K. Geiger.